Numerical Study of a Gas Bubble Rising Through Stagnant Fluid

Eliandro R. Cirilo, eliandro.cirilo@gmail.com
Antonio Castelo Filho, antonio.castelo.filho@gmail.com
Departamento de Cincias de Computao e Estatstica, Instituto de Cincias Matemticas e de Computao, Universidade de So Paulo, Avenida Trabalhador so-carlense 400, Caixa Postal 668, CEP 13560-970 So Carlos, SP, Brazil

Abstract. *It is well known that the environment degradation has come along the time positioning as one of the main problems from modern world. Among several questions of the environmental interest the methane bubble rise in the lakes can be emphasized, from the anoxic sediment in the bottom of lake until water interface atmosphere. In particular, the present academic work has come to treat mathematic modeling of the bubble rise through sediment viscous fluid near the bottom lake and present results, via Mathematics and Computing-Numeric Simulation, about the terminal velocity ascent of the bubble.*

Keywords: *environmental, fluid flow, bubble rise, mathematic modeling, numerical simulation*

1. INTRODUCTION

The motion of the a single bubble has been studied by several researchers, then this problem promotes research in areas such as experimental, numerical and quantification. Many monographs, articles and technical papers come over the last years being done in order to describe the details of this movement. To understand the velocity's rise, the shape, the path traveled and others questions, for various types of the fluids, it is important in a infinity of the applied problems of the sciences.

For example, the bubble rising freely in quiescent non-newtonian viscous inelastic fluids was investigated experimentally and computationally by Zhang *et al.* (2010). There, the autors demonstrated that the comparison of the experimental measurements of terminal bubble shape and velocity with the computational results are satisfactory, when the fluid was shear-thinning. Experimentaly, Shew and Pinton (2006) investigated the dynamics of millimetric size air bubbles rising through a still 1% polyacrylamide/water solution. They compared the oscillatory path of the bubble with those bubbles rising in water and they found changes in path geometry, the onset of path instability, as well as lift forces. They said that the observed effects are attributed to viscoelastic effects in the wake of the bubble. To simulate bubble motion in newtonian and viscoelastic fluids have been investigated too. Jiménez *et al.* (2005), studing axisymmetric gas-liquid systems, compared the computational results with experimental results. They shown in their work the dynamics of a gas bubble bursting a free surface of a newtonian and viscoelastic fluid. Majumder *et al.* (2005) developed a theoretical model for predicting dynamic behaviour of bubble dispersion at plunging region in an ejector induced downflow bubble column reactor. The model of their work is able to simulate the instantaneous growing shape of bubble during its formation and determine the final size of detachment at plunging point of liquid jet in incompressible newtonian and non-newtonian fluids. For situation of the ionic liquids, Wang *et al.* (2010) simulate the motion of single bubble. They used in your simulations three ionic liquids, i.e., bmimBF4, bmimPF6 and omimBF4, and the calculation results agree well with the experimental data. This work was important for understanding the fluid dynamic performance of bubbles in ionic liquids, and could provide a useful tool for designing a bubble column with ionic liquids as its solvents. The buoyancy and drag forces are strongly dependent on fluid properties of gravity and equivalent diameter, when a bubble ascend in a liquid column. Talaia (2007) showed that bubble's rise terminal velocity is strongly dependent on dynamic viscosity effect. For this, he studied a set of bubble rising velocity experiments in a liquid column using water or glycerol. The data set allowed to have some terminal velocities data interval of $8.0 - 32.9cm/s$ with Reynolds number interval $1.3 - 7490$.

In the case of numerical context, Barkhudarov and Chin (1994) analysed the numerical stability of the free-surface-tracking algorithm based on the SOLA-VOF method when modelling gas bubble evolution in a fluid. The code for simulating incompressible, imiscible, unsteady, Newtonian, multi-fluid flows with free surfaces was building by Sousa *et al.* (2004). The numerical method of them is based on the GENSMAC-3D front-tracking method. The free-surface and the interfaces are represented by an unstructured Lagrangian grid moving through an Eulerian grid. Complex numerical simulations such as two bubbles rising in a container was realized, showing the capability and robustness of method. Annaland *et al.* (2005) in your paper, propose a hybrid model for the numerical simulation of gas-liquid-solid flows using a combined front tracking and discrete particle approach applied for, respectively, dispersed gas bubbles and solid particles present in the continuous liquid phase. In this work was studied the effect of the volumetric particle concentration and retard effect on the bubble rise velocity due to the presence of the suspended solid particles.

In the environmental scope, some scientific papers have the aim to investigate the methane's transport from sediments to water bodies via bubbles. Methane plays an important role in the atmosphere as a greenhouse gas. Louis *et al.* (2000) says that methane bubbles contribute significantly to greenhouse gas fluxes because they are a direct conduit of CH_4

from sediments to the atmosphere, escaping microbial oxidation. The contribution of lakes and swamps to the total methane flux to the atmosphere is about 25% (Makhov and Bazhin, 1999). McGinnis *et al.* (2006) quantified methane gas bubble dissolution using bubble modeling and acoustic observations of rising bubbles to determine what fraction of the methane transported by bubbles will reach the atmosphere. The quantity of methane produced by sediments of Wintergreen Lake was measured by Strayer and Tiedje (1978). There, they measured methane by ebullition (using bubble traps) and estimating methane in the water column by diffusion. Bastviken *et al.* (2004) says in your work that lakes sediments are critical's points of methane production, and the methane can be exported from the sediment either by ebullition or by diffusion. They explain that ebullition results in direct flux of methane from the sediment to the atmosphere, with limited impact of methane oxidation in the water column. For this work they took data of the 11 North American and 13 Swedish lakes, and literature values from 49 lakes.

According to what was exposed, we propose in this work to model and simulate the fluid flow around of the air and methane spherical bubbles, in a axisymmetric computational grid that models the domain located near the bottom of a lake. The equations which governing flow field are discretized by a finites differences approximations on a stationary grid, and a bubble moves through the stationary grid. Thus, we would describe the initials characteristics of the bubble's rise to environmental interest.

The rest of this work proceeds organized as it follows. In the section 2 we present the studied domain, the governing equations, initial and boundary conditions, nondimensionals, appropriate to the mathematical model. In the section 3 we show the main steps of the calculation from our code and comment on the methodology applied in the numerical discretization of the computational mesh and of the equations. In the section 4 we display a set of simulations comparing our results with the literature in the air-water system. This allowed us to simulate the cases in the methane-water and methane-near the sediment systems. In the section 5 we conclude about the work developed and suggest a study future for the rise of the bubble. Finally we make the acknowledgments.

2. MATEMATICAL FORMULATION

The motion of bubble inside the fluid is considered axisymmetric in (r, z) coordinates system. In our model we consider that the laws governing the buoyancy of a gas bubble in an incompressible newtonian fluid are:

$$\nabla . V = 0 \tag{1}$$

$$\rho \frac{DV}{Dt} = \nabla . \underline{\underline{\sigma}} + \rho G \tag{2}$$

$$F = m . \frac{dV_c}{dt} \tag{3}$$

this model D/Dt, d/dt are material and temporal derivatives; $\underline{\underline{\sigma}}$ is the viscous stress tensor; V, V_c , G and F are vectors velocity, mass's center velocity, gravity and resultant of forces; and finally ρ, m are constants density and mass. The Eq. (1), Eq. (2) governing to motion of the fluid and Eq. (3) the ascend motion of the bubble.

The domain studied in this work is shown in Fig. 1. The N_g, P_g are the viscosity and density of gas and N_f, P_f are the viscosity and density of the fluid around of the bubble, finally R and H are the dimensions horizontal and vertical respectively.

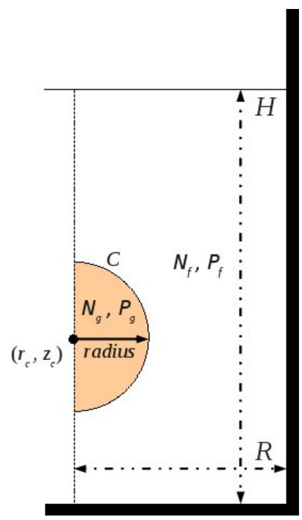

Figure 1. Geometry used.

Let L, U, N and P denote length, velocity, viscosity and density scales and consider the nondimensionalization below, where g_i is the gravity component and g_0 the constant.

$$\begin{array}{lllllll} r = L\bar{r} & z = L\bar{z} & u = U\bar{u} & v = U\bar{v} & \rho = P\bar{\rho} & t = \frac{L}{U}\bar{t} & p = PU^2\bar{p} \\ vol = L^3\bar{vol} & E = L^2P_fU^2\bar{E} & W = L^2P_gU^2\bar{W} & g_i = g_0\bar{g}_i & & & \end{array}$$

Introducing nondimensionalization into Eq. (1), Eq. (2) the equations describing fluid field around bubble may be written as:

$$\frac{1}{\bar{r}}\frac{\partial \bar{r}\bar{u}}{\partial \bar{r}} + \frac{\partial \bar{v}}{\partial \bar{z}} = 0 \tag{4}$$

$$\frac{\partial \bar{u}}{\partial \bar{t}} + \frac{1}{\bar{r}}\frac{\partial \bar{r}\bar{u}\bar{u}}{\partial \bar{r}} + \frac{\partial \bar{u}\bar{v}}{\partial \bar{z}} = -\frac{\partial \bar{p}}{\partial \bar{r}} + \frac{1}{Re}\left[\frac{1}{\bar{r}}\frac{\partial}{\partial \bar{r}}\left(\bar{r}\frac{\partial \bar{u}}{\partial \bar{r}}\right) + \frac{\partial^2 \bar{u}}{\partial \bar{z}^2} - \frac{\bar{u}}{\bar{r}^2}\right] + \frac{1}{Fr}\bar{g}_r \tag{5}$$

$$\frac{\partial \bar{v}}{\partial \bar{t}} + \frac{1}{\bar{r}}\frac{\partial \bar{r}\bar{v}\bar{u}}{\partial \bar{r}} + \frac{\partial \bar{v}\bar{v}}{\partial \bar{z}} = -\frac{\partial \bar{p}}{\partial \bar{z}} + \frac{1}{Re}\left[\frac{1}{\bar{r}}\frac{\partial}{\partial \bar{r}}\left(\bar{r}\frac{\partial \bar{v}}{\partial \bar{r}}\right) + \frac{\partial^2 \bar{v}}{\partial \bar{z}^2}\right] + \frac{1}{Fr}\bar{g}_z \tag{6}$$

so that $Re = UL/N$, $Fr = U^2/Lg_0$ are the associated Reynolds number and Froude number, respectively.

The rise of bubble is due the empuxo (E), weight (W) and viscous force (FV), thus Newton's second law (Eq. (3)) we have that the move the center mass (r_c, z_c) of the bubble is given from the following expressions:

$$\frac{d\bar{u}_c}{d\bar{t}} = \frac{1}{\bar{\rho}_g\bar{vol}}\left[\bar{FV}_r\right] \qquad , \frac{d\bar{r}_c}{d\bar{t}} = \bar{u}_c \tag{7}$$

$$\frac{d\bar{v}_c}{d\bar{t}} = \frac{1}{\bar{\rho}_g\bar{vol}}\left[\bar{E} + \bar{W} + \bar{FV}_z\right] \qquad , \frac{d\bar{z}_c}{d\bar{t}} = \bar{v}_c \tag{8}$$

with $\bar{vol}$ being the nondimensional volume of the bubble, $\bar{E} = -(1/Fr)\bar{\rho}_f\bar{g}_z\bar{vol}$ and $\bar{W} = (1/Fr)\bar{\rho}_g\bar{g}_z\bar{vol}$.

The $\bar{FV}$ act throughout surface (C), Fig. 1, through it occurs the coupling among the equations Eq. (1), Eq. (2) and Eq. (3). It is given as (Pontes, 1999):

$$\bar{FV} = \int_C \underline{\underline{\bar{\sigma}}}.\mathbf{n}dl \tag{9}$$

and $\underline{\underline{\bar{\sigma}}}.\mathbf{n}$ is such that

$$\begin{pmatrix} -\bar{p} + \frac{2}{Re}\frac{\partial \bar{u}}{\partial \bar{r}} & 0 & \frac{1}{Re}\left[\frac{\partial \bar{u}}{\partial \bar{z}} + \frac{\partial \bar{v}}{\partial \bar{r}}\right] \\ 0 & -\bar{p} + \frac{2}{Re}\frac{\bar{u}}{\bar{r}} & 0 \\ \frac{1}{Re}\left[\frac{\partial \bar{u}}{\partial \bar{z}} + \frac{\partial \bar{v}}{\partial \bar{r}}\right] & 0 & -\bar{p} + \frac{2}{Re}\frac{\partial \bar{v}}{\partial \bar{z}} \end{pmatrix} . \begin{pmatrix} n_1 \\ 0 \\ n_3 \end{pmatrix} = \begin{pmatrix} \left[-\bar{p} + \frac{2}{Re}\frac{\partial \bar{u}}{\partial \bar{r}}\right]n_1 + \frac{1}{Re}\left[\frac{\partial \bar{u}}{\partial \bar{z}} + \frac{\partial \bar{v}}{\partial \bar{r}}\right]n_3 \\ 0 \\ \frac{1}{Re}\left[\frac{\partial \bar{u}}{\partial \bar{z}} + \frac{\partial \bar{v}}{\partial \bar{r}}\right]n_1 + \left[-\bar{p} + \frac{2}{Re}\frac{\partial \bar{v}}{\partial \bar{z}}\right]n_3 \end{pmatrix}$$

It is important to note that FV_r is null, resulting in $\bar{u}_c = 0$, because the problem is considered in axisymmetric system. The viscous force in direction z is given as follows

$$FV_z = \int_C \left(\frac{1}{Re}\left[\frac{\partial \bar{u}}{\partial \bar{z}} + \frac{\partial \bar{v}}{\partial \bar{r}}\right]n_1 + \left[-\bar{p} + \frac{2}{Re}\frac{\partial \bar{v}}{\partial \bar{z}}\right]n_3\right)dl \tag{10}$$

The initial condition is

$$\bar{V}^0 = \begin{pmatrix} \bar{u} \\ \bar{v} \end{pmatrix} = \begin{pmatrix} 0 \\ 0 \end{pmatrix} \quad , \quad 0 \le \bar{r} \le \bar{R} \quad , \quad 0 \le \bar{z} \le \bar{H} \quad , \quad \bar{t} = 0 \tag{11}$$

and no-slip boundary conditions on the container walls are implemented by

$$\bar{V}^{\bar{t}} = \begin{pmatrix} \bar{u} \\ \bar{v} \end{pmatrix} = \begin{pmatrix} 0 \\ 0 \end{pmatrix} \quad , \quad \begin{cases} 0 \le \bar{r} \le \bar{R} & , \quad \bar{z} = 0 \quad , \quad \bar{t} > 0 \\ 0 \le \bar{z} \le \bar{H} & , \quad \bar{r} = \bar{R} \quad , \quad \bar{t} > 0 \end{cases} \tag{12}$$

At the free surface, with absence of surface tension, the boundary condition is such that,

$$\begin{array}{l} -\bar{p} + \frac{2}{Re}\left[\frac{\partial \bar{u}}{\partial \bar{r}}n_1^2 + \left(\frac{\partial \bar{u}}{\partial \bar{z}} + \frac{\partial \bar{v}}{\partial \bar{r}}\right)n_1n_3 + \frac{\partial \bar{v}}{\partial \bar{z}}n_3^2\right] = 0 \\ \left(\frac{\partial \bar{u}}{\partial \bar{z}} + \frac{\partial \bar{v}}{\partial \bar{r}}\right)(n_1^2 - n_3^2) + 2\left(\frac{\partial \bar{v}}{\partial \bar{z}} - \frac{\partial \bar{u}}{\partial \bar{r}}\right)n_1n_3 = 0 \end{array} \quad , \quad 0 \le \bar{r} \le \bar{R} \quad , \quad \bar{z} = \bar{H} \quad , \quad \bar{t} > 0 \tag{13}$$

We considered the free surface as a boundary condition because the ascent of the bubble can not move it. If it occurs we will increase the vertical dimension, hoping that the free surface does not move. We want to impose boundary conditions that simulate the rise in an infinite medium.

From the assumption of axial symmetry, then

$$\bar{u}=0 \quad , \quad \frac{\partial \bar{v}}{\partial \bar{r}}=0 \quad ,0 \leq \bar{z} \leq \bar{H} \quad , \quad \bar{r}=0 \quad , \quad \bar{t}>0 \tag{14}$$

So, our mathematical model is given by system of equations Eq. (4), Eq. (5), Eq. (6), Eq. (8) and Eq. (10) subject to conditions Eq. (11) - Eq. (14), and a computer code was developed in C language to solve the mathematical model numerically.

3. NUMERICAL METHODOLOGY

The problem of this work was solved based on FREEFLOW-AXI code developed by Oliveira (2002). There, the code solves the equations Eq. (4), Eq. (5), Eq. (6) by Projection Method. It was prepared for solving only axisymmetric free surface flows applying GENSMAC (Generalized-Simplified-Marker-and-Cell) method developed by Tomé and McKee (1994). We extend the code to solve immersed bodies problems in a fluid pool where the body interacts with the fluid.

In our code, to solve Eq. (4), Eq. (5), Eq. (6), Eq. (8) and (10), we assume that in a given time $\bar{t}_0$, the velocity field $\bar{V}^{\bar{t}_0}$ is known, boundary conditions for the velocity and pressure are given, and the mass center of the bubble is know too. To compute the velocity field, the pressure field and bubble's positon at the advanced time $\bar{t}=\bar{t}_0+\bar{\delta}t$, we proceed as it follows:

1. Let $\left(\tilde{\bar{p}}\right)^{\bar{t}_0}$ be a pressure field which satisfies the correct pressure condition on the free surface.

2. Calculate the intermediate velocity field $\tilde{\tilde{\bar{V}}}$ from

$$\frac{\partial}{\partial \bar{t}}\left(\tilde{\tilde{\bar{V}}}\right)=-\nabla\tilde{\bar{p}}-\nabla.\left(\tilde{\tilde{\bar{V}}}\tilde{\tilde{\bar{V}}}\right)+\frac{1}{Re}\left[\nabla\tilde{\tilde{\bar{V}}}+\left(\nabla\tilde{\tilde{\bar{V}}}\right)^T\right]+\frac{1}{Fr}\bar{G} \tag{15}$$

with $\left(\tilde{\tilde{\bar{V}}}\right)^{t_0}=\left(\bar{V}\right)^{t_0}$ (correct boundary conditions).

3. Solve the Poisson equation (Tomé *et al.*, 1996b) to the scalar function $\psi\left(r,z,t\right)$

$$\nabla^2\psi=\nabla.\tilde{\tilde{\bar{V}}} \tag{16}$$

where the boundary conditions are $\partial\psi/\partial n=0$ on rigid boundaries and $\psi=0$ on the free surface.

4. Compute the velocity field updated

$$\bar{V}=\tilde{\tilde{\bar{V}}}-\nabla\psi \tag{17}$$

5. Compute the pressure by

$$\bar{p}=\tilde{\bar{p}}+\frac{1}{\bar{\delta}t}\psi \tag{18}$$

6. Compute the viscous force FV_z, Eqs. (10).

7. Update position and velocity of the mass center, simulating the bubble's move. This is done by solving Eqs. (8).

8. Update the markers positions, solving

$$\frac{d\bar{r}}{d\bar{t}}=\bar{u} \quad , \quad \frac{d\bar{z}}{d\bar{t}}=\bar{v} \tag{19}$$

this step is to movement the markers to their new positions (Oliveira, 2002). This results of methodology to solve problems of free surface flows.

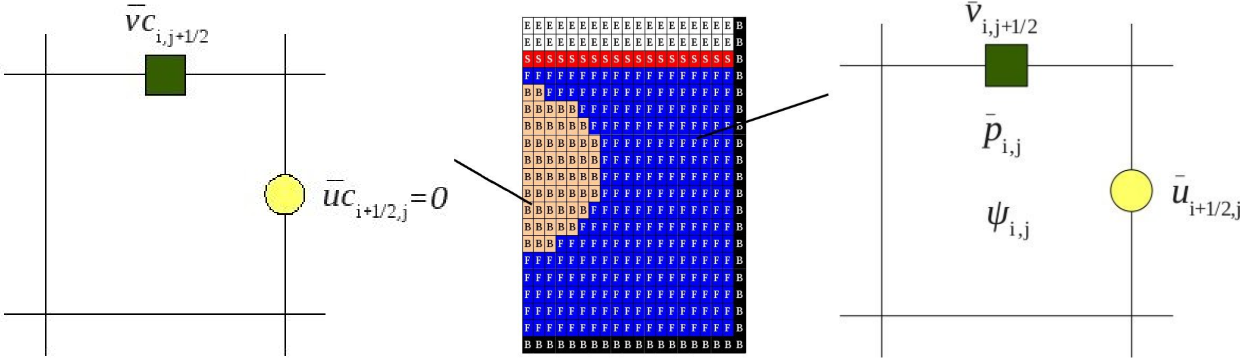

Figure 2. Bubble's cell (left), computational grid (middle) and fluid's cell (right).

A scheme for identifying the free surface, boundary and the fluid region is employed. To accommodate this, the cells within the mesh are defined as full cells (F), surface cells (S), empty cells (E) and boundary cells (B), Fig. 2 middle. A detailed description of these is given by (Tomé *et al.*, 2001). Our model equations is solved by a finite difference method on the cartesian grid (Fig. 2 middle), which dimension of the cell is $\bar{\delta r} \times \bar{\delta z}$ where $\bar{\delta r} \equiv \bar{\delta z}$.

As can be seen in the Fig. 2 right, the variables $\bar{p}_{i,j}$, $\psi_{i,j}$ are positioned at a cell center, while $\bar{u}_{i,j}$, $\bar{v}_{i,j}$ are staggered by a translation of $\bar{\delta r}/2$, $\bar{\delta z}/2$ respectively. This it is reason of the label $\bar{u}_{i+1/2,j}$, $\bar{v}_{i,j+1/2}$.

In case of the boundary cells (B), those (B) in black are the rigid boundary and the condition no-slip Eq. (12) is employed. But the cells (B) in orange assumes the bubble's velocity $\bar{u}_c$, $\bar{v}_c$, Fig. 2 left. Here $\bar{u}_c = 0$ and $\bar{v}_c$ is calculated by step 7, it closes the question about the boundary conditions for our problem.

More precisely, the Eq. (15) is solved by explicit Euler method (Fortuna, 2000) in faces $(i + 1/2, j)$ and $(i, j + 1/2)$, in order to correct $\bar{u}_{i+1/2,j}$, $\bar{v}_{i,j+1/2}$ soon by Eq. (17). The convective term is approximated by a high order upwind scheme namely SDPUS (Lima, 2010), and diffusive and pressure terms are approximated by central differences.

The Eq. (16) consists in a sparse symmetric system, the discrete Poisson equation, then it is solved by conjugate gradient method. Poisson's equation has error of the order $O(h^2)$ ($h = \bar{\delta r} \equiv \bar{\delta z}$), so that halving the stepsize roughly reduces the error by a factor of four (Griebel *et al.*, 1997).

Ownership velocity $\bar{u}_{i+1/2,j}$, $\bar{v}_{i,j+1/2}$ and pressure $\bar{p}_{i,j}$ of the fluid, the force FV_z, in the step 6, is calculated and the system Eqs. (8) is solved by Euler method, providing translation of the bubble. Of course, appropriated boundary conditions are implemented in the border C. Observing the Fig. 3 right, the cells (F) in green were type (B), see Fig. 3 left, but these cells (F) do not have prescribe velocity in the current time. Then, we attribute bubble's velocity these cells. Similarly, this idea occurs about the cells (B) in green. Here we have the effect of the coupling between fluid's equations and bubble's equations. We emphasize that these things, and its details, were incorporated to FREEFLOW-AXI for to simulate the slice's move immersed in the fluid containers.

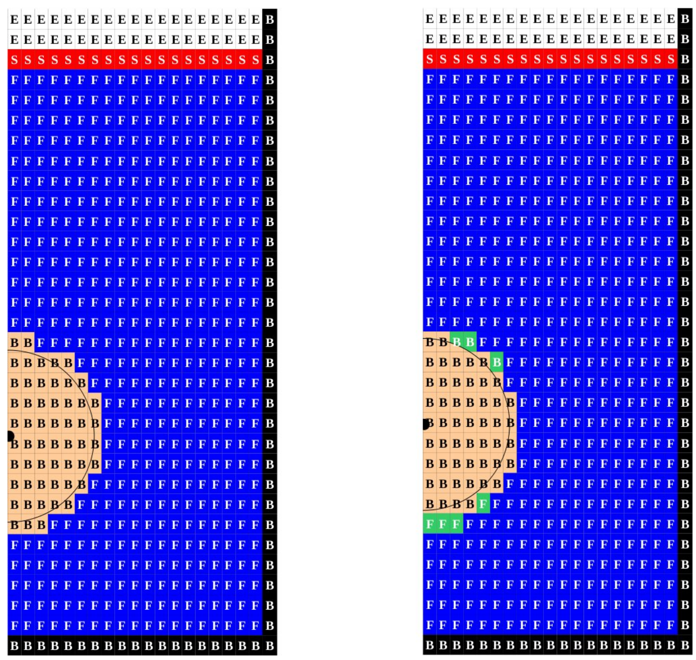

Figure 3. Left - Types of cells used in the Code. Right - Bubble's displacement and news labels for cells

Finally the Eqs. (19) are solved by Euler method too, then the update the markers positions is realized. For more details about marker particles see Tomé *et al.* (1996a).

4. RESULTS AND DISCUSSION

4.1 Validation of numerical predictions

The Bubble's nondimensional parameters employed in this work are, Reynolds number (Re_B) and Bond number (Bo_B). The dimensionless numbers are defined as:

$$Re_B = \frac{Dv_c^T}{\nu_f} \quad , \quad Bo_B = \frac{g_0\left(\rho_f - \rho_g\right)D^2}{\sigma} \tag{20}$$

here D and v_c^T are bubble's diameter and terminal velocity of the mass center respectively, and σ is the surface tension.

Mukundakrishnan *et al.* (2007) studied the size of the solution domain ($R \times H$) for cases spherical and spherical-cap-skirted bubbles. They explains that the wall effects are noted when the dimensions of the channel are reduced from a given values. The Bubble's Reynolds number decreases when reduce is made, then the terminal velocity of mass center can be not realistic. So, they employed in yours simulations $R \geq 6D$ and $H \geq 3D$. They concluded that the bubble motion results in the attainment of terminal velocity values and shapes corresponding to those in an infinite medium. On the path followed, Wua and Gharib (2002) illustrated that bubbles with diameter less than about 0.15 centimeters rise rectilinearly. In this work, they showed that nearly spherical bubbles, with diameter 1.11 milimeters, travel straight path and switches to a zigzag path when the bubble diameter exceeds 0.15 cm or Reynolds number exceeds 280.

Table 1. Data set to simulations.

$Domain$	$R^{(1)}$	$H^{(1)}$	$grid$
S_1	3.0	21.0	30×210
S_2	6.0	21.0	60×210
S_3	9.0	12.0	90×120
S_4	9.0	21.0	90×210
S_5	9.0	42.0	90×420
S_6	14.0	32.0	140×320

$Bubbles$	$D^{(1)}$	$Systems$
B_1	1.0	*air/water*
B_2	1.0	*methane/water*
B_3	1.0	*methane/near the sediment*
B_4	1.5	*air/water*
B_5	1.5	*methane/water*
B_6	1.5	*methane/near the sediment*

$^{(1)}$: measured at milimeters

Considering the previous information we performed a set simulations whose data are shown in Tab. 1. A simulation is the union of the lines between tables left and right respectively. To simulations $\{S_i; B_1\}$ ($i = 1, 2, 3, 4, 5$) us use $Bo_B \approx 0.13$ and at $\{S_6; B_4\}$ $Bo_B \approx 0.3$ with $Re_B < 300$ at all simulations. Then, according to the map of Fig. 4 our simulations fits into the rise of a spherical bubble.

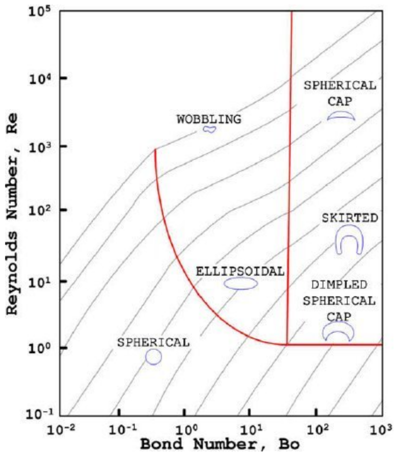

Figure 4. Shapes of air bubbles rising in water (Clift *et al.*, 2005).

Note at Tab. 1 that the values R and H satisfy $R \geq 6D$ and $H \geq 3D$ to simulations, however the value R for $\{S_1; B_1\}$ is not verified. Look that the variation in R causes the appearance of the wall effects, see Fig. 5 left. Analogously the variation in H causes it too, see Fig. 5 middle, but it at low intensity.

Observing the bubble's velocity of the set data $\{S_4; B_1\}$ and $\{S_5; B_1\}$, Fig. 5 right, we conclude a close proximity between the velocity profiles. Then considering the profile from $\{S_4; B_1\}$ as numerical solution and comparing it with

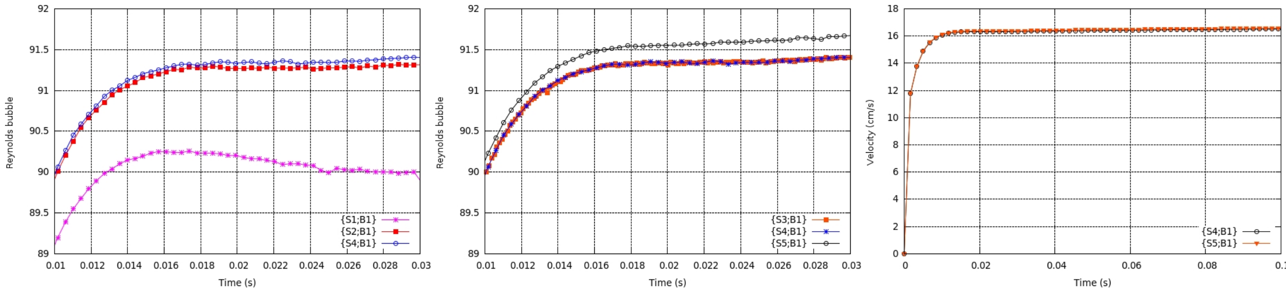

Figure 5. Bubble's Reynolds to simulations (left), (middle) and Bubble's velocity (right).

the solution obtained by Xu and Guetari (2004), look Fig. 6 left, we conclude that results are in good agreement. This displays that our method is able to simulate the bubble buoyance.

Clift *et al.* (2005) calculated experimentally the terminal velocity for spherical bubble with diameter $D = 1.5mm$, and Nadooshan and Shirani (2008) used the actual densities of air and water for this bubble obtaining results in close agreement with the experimental data. Using the set data $\{S_6; B_4\}$ and these actual densities, but nondimensionals, we compared the rise velocity, see Fig. 6 right. Good agreement between results was observed too. This prompted us to evaluate the behavior of the bubble velocity in a more viscous fluid, which is one of the objects of our investigation.

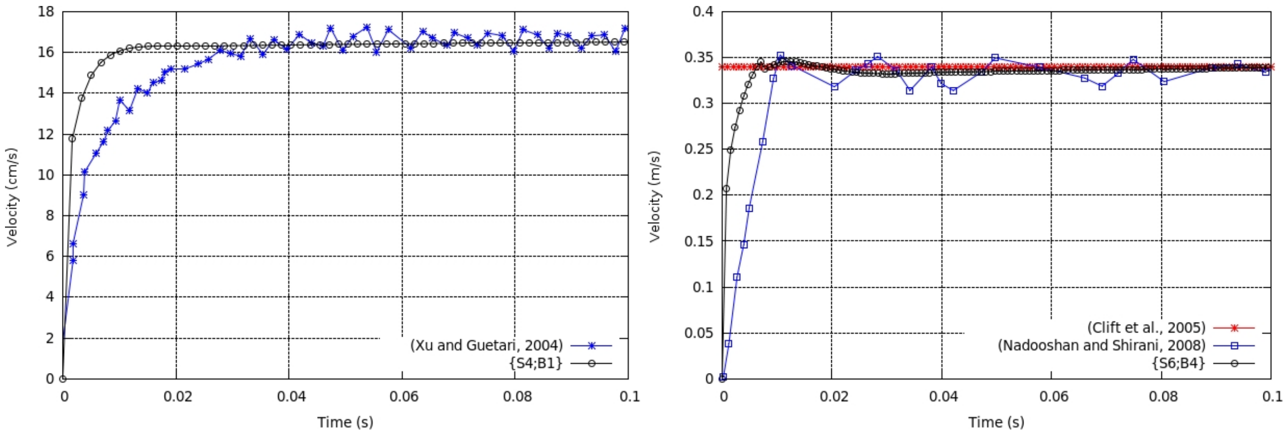

Figure 6. Bubble velocity for $D = 1.0mm$ (left) and $D = 1.5mm$ (right).

4.2 Aplication of numerical predictions

Typically the bottom's lakes is considered without oxygen (anoxic), this location takes place the biological process called methanogenesis by microorganisms methanogenic Archaea (Strayer and Tiedje, 1978). Methanogenesis is the process organic matter degradation to methane (Oremland, 1988). The Bubble's methane formation is expected at the bottom's lakes in conditions favoring the occurrence of methanogenesis. When there are high rates of methane production and it is greater than the rate of vertical diffusion of methane, which occurs toward the sediment-water interface, this gives an increase of supersaturation of the gas and thus appears the bubble of methane (Louis *et al.*, 2000). Abe *et al.* (2005) measured methane in sediments of the Lobo-Broa Reservoir. In this lake they observed that, when the gas exceeded its *in situ* gas saturation value at this shallow water depths, resulting in numerous sediment bubbles, analogously the Louis *et al.* (2000). Even though the Lobo-Broa Reservoir is classified as oligotrophic (low amount of nutrients in the sediment), the sediment gas concentrations were high.

According to the facts mentioned in the previous paragraph, we believe that is important to know the rise of the bubble of methane near the sediment. Under these conditions, we consider a bubble that has been formed and that it is in the water but near to the sediment. To simulate this situation was considered a fluid as water and another two times more viscous than water. The simulations occurred for data $\{S_4; B_i\}$-$\{S_6; B_j\}$ $(i = 1, 2, 3; j = 4, 5, 6)$ from Tab. 1, the number Bo_B is approximately the same as above and Re_B is smaller than the one above too.

Looking the graphic of the Fig. 7 (left) to sets $\{S_4; B_1\}$ and $\{S_4; B_2\}$, can be concluded that the rise velocity of bubbles air and methane are very similar, even though the methane density be close to $60, 45\%$ of the air density. Can be also noted that bubble's velocity of methane is minor when immersed at fluid whose viscosity is two times more than water, see velocity's profiles of the sets $\{S_4; B_2\}$ and $\{S_4; B_3\}$ in same figure. Analogously, it is observed too in case of a bubble greater, Fig. 7 (right).

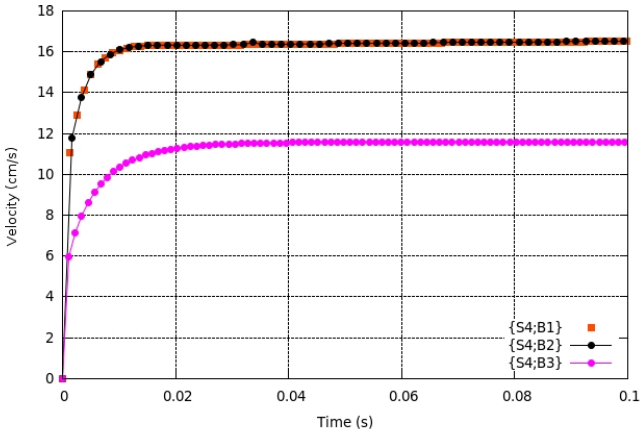

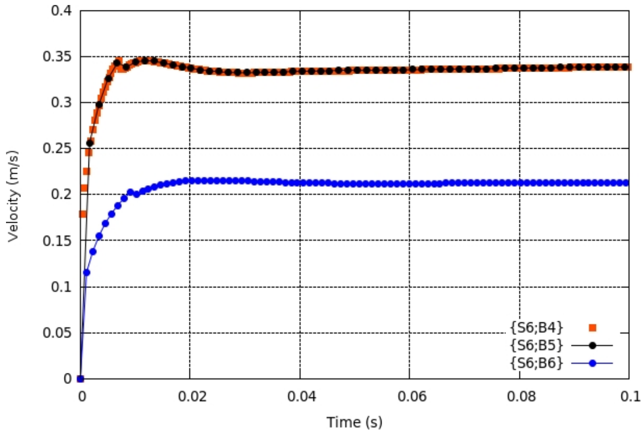

Figure 7. Bubble velocity for $D = 1.0mm$ (left) and $D = 1.5mm$ (right).

This shows that to amend at viscosity changes strongly the ascend velocity. In this aplication, we considered the viscosity of the fluid two times more than water because it is next to lake bottom. It is known that a fluid with a small concentration of sediment remains with newtonian properties and may make changes in its viscosity; when the sediment concentration increases, the mixture ceases to behave as Newtonian, giving then non-Newtonian properties (Santos *et al.*, 2003).

Summarizing, was admitted a *Nepheloid layer* (Nepheloid layer is a layer of water that contains significant amounts of suspended sediment) of the fluid whose profusion of sedimentary particles, with negligible size, are distributed throughout the fluid and this alters the viscosity. This feature is appropriate for the fluid and some papers has discussed this fact. For example, Belinsky *et al.* (2005) performed experiments and simulations in order to characterize the distributions of concentrations of suspended particulate matter in water columns of lakes and reservoirs. In this work they concluded that the distribution of suspended particulate matter exhibited a layer near the bottom, that is thought to be analogous to the benthic nepheloid layer observed in larger lakes.

5. CONCLUSION

In this paper, a nondimensional model to simulate the rise of an axisymmetric spherical bubble was presented. The model proved to be a simple alternative when compared to that presented by (Annaland *et al.*, 2005) and (Sousa *et al.*, 2004). We presented a finite difference technique for solving the fluid field around bubble combined with Newton's second law that move mass's center (r_c, z_c) and consequently simulate the bubble's movement. This technique proved to be able to simulate the rise of the bubble for a set of the cases. To this, we compared our results with those in existing literature. Besides we simulated the situation of to ascend methane's bubble immers at fluid more viscous than water and next to lake bottom. We showed that this fluid amends appreciably the ascend velocity, because a small particle concentration changes the viscosity. We emphasize that the alteration in viscosity, with the intention to consider a concentration of sedimentary particles suspended in water, showed a significant change in the bubble rise velocity, and it is in accordance with the work of Talaia (2007) and Annaland *et al.* (2005).

This study shows the need to investigate the fluid when the concentration of sedimentary particles is appreciable, because the fluid is non-newtonian. Therefore, in a future study buoyance's effects of the bubble in a non-newtonian fluids will be explored.

6. ACKNOWLEDGEMENTS

The authors gratefully acknowledge CNPq Grant No. 141174/2009-9 for supporting this study.

7. REFERENCES

Abe, D.S., Adams, D.D., Galli, C.V.S., Sikar, E. and Tundisi, J.G., 2005. "Sediment greenhouse gases (methane and carbon dioxide) in the lobo-broa reservoir, são paulo state, brazil: Concentrations and diffuse emission fluxes for carbon budget considerations". *Lakes and Reservoirs: Research and Management*, Vol. 10, pp. 201–209.

Annaland, M.S., Deen, N.G. and Kuipers, J.A.M., 2005. "Numerical simulation of gas-liquid-solid flows using a combined front tracking and discrete particle method". *Chemical Engineering Science*, Vol. 60, pp. 6188–6198.

Barkhudarov, M.R. and Chin, S.B., 1994. "Stability of a numerical algorithm for gas bubble modelling". *International Journal for Numerical Methods in Fluids*, Vol. 19, pp. 415–437.

Bastviken, D., Cole, J., Pace, M. and Tranvik, L., 2004. "Methane emissions from lakes: Dependence of lake characteristics, two regional assessments, and a global estimate". *Global Biogeochemical Cycles*, Vol. 18, pp. 1–12.

Belinsky, M., Rubin, H., Agnon, Y., Kit, E. and Atkinson, J.F., 2005. "Characteristics of resuspension, settling and diffusion of particulate matter in a water column". *Environmental Fluid Mechanics*, Vol. 5, pp. 415–441.

Clift, R., Grace, J.R. and Weber, M.E., 2005. *Bubbles, Drops, and Particles*. Dover Publications, New York, USA.

Fortuna, A.O., 2000. *Tecnicas Computacionais Para Dinamica Dos Fluidos*. Ed. Edusp, São Paulo, Brazil.

Griebel, M., Dornseifer, T. and Neunhoeffer, T., 1997. *Numerical Simulation in Fluid Dynamics: a practical introduction*. Ed. SIAM, Philadelphia, USA.

Jiménez, E., Sussman, M. and Ohta, M., 2005. "A computational study of bubble motion in newtonian and viscoelastic fluids". *Journal of Statistical Mechanics: Theory and Experiment*, Vol. 1, pp. 97–107.

Lima, G.A.B., 2010. *Desenvolvimento de estratégias de captura de descontinuidades para leis de conservação e problemas relacionados em dinâmica dos fluidos*. Ph.D. thesis, Universidade de São Paulo, São Carlos, SP, Brasil.

Louis, V.L.S., Kelly, C.A., Duchemin, É., Rudd, J.W.M. and Rosenberg, D.M., 2000. "Reservoir surfaces as sources of greenhouse gases to the atmosphere: A global estimate". *BioScience*, Vol. 50, pp. 766–775.

Majumder, S.K., Kundu, G. and Mukherjee, D., 2005. "Theoretical study of bubble motion due to pressure distribution and energy dissipation in plunging liquid jet downflow bubble column". *Institution of Engineerings (India) Journal - CH*, Vol. 86, pp. 29–33.

Makhov, G.A. and Bazhin, N.M., 1999. "Methane emission from lakes". *Chemosphere*, Vol. 38, pp. 1453–1459.

McGinnis, D.F., Greinert, J., Artemov, Y., Beaubien, S.E. and Wüest, A., 2006. "Fate of rising methane bubbles in stratified waters: How much methane reaches the atmosphere?" *Journal of Geophysical Research*, Vol. 111, pp. 1–15.

Mukundakrishnan, K., Quan, S., Ayyaswamy, P.S. and Eckmann, D.M., 2007. "Numerical study of wall effects on buoyant gas-bubble rise in a liquid-filled finite cylinder". *Physical Review E*, Vol. 76, pp. 1–15.

Nadooshan, A.A. and Shirani, E., 2008. "Numerical simulation of a single air bubble rising in water with various models of surface tension force". *World Academy of Science, Engineering and Technology*, Vol. 39, pp. 72–76.

Oliveira, M.L.B., 2002. *Freeflow-Axi: Um ambiente de simulação de escoamentos axissimétricos com superfícies livres*. Ph.D. thesis, Universidade de São Paulo, São Carlos, SP, Brasil.

Oremland, R.C., 1988. *Biogeochemistry of methanogenic bacteria. In: Biology of anaerobic microorganisms*. John Wiley and Sons, New York, USA.

Pontes, J., 1999. "Fenômenos de transferência". Technical Reports, COPPE/UFRJ.

Santos, F.L., Maciel, G.F. and Moraes, V.M., 2003. "Evolução de frentes de lama em canais - parte i: Uma proposta reológica de herschel-bulkley a partir de uma base experimentalista física". *RBRH - Revista Brasileira de Recursos Hídricos*, Vol. 8, pp. 95–105.

Shew, W.L. and Pinton, J.F., 2006. "Viscoelastic effects on the dynamics of a rising bubble". *Journal of Statistical Mechanics: Theory and Experiment*, Vol. 206, pp. 1–17.

Sousa, F.S., Mangiavacchi, N., Nonato, L.G., Castelo, A., Tomé, M.F., Ferreira, V.G. and McKee, J.A.C.S., 2004. "A front-tracking/front-capturing method for the simulation of 3d multi-fluid flows with free surfaces". *Journal of Computational Physics*, Vol. 198, pp. 469–499.

Strayer, R.F. and Tiedje, J.M., 1978. "In situ methane production in a small, hypereutrophic, hard-water lake: Loss of methane from sediments by vertical diffusion and ebullition". *Limnol. Oceanogr.*, Vol. 23, pp. 1201–1206.

Talaia, M.A.R., 2007. "Terminal velocity of a bubble rise in a liquid column". In *Proceedings of World Academy of Science, Engineering and Technology*. ISSN 1307-6884, Vol. 22, pp. 264–268.

Tomé, M.F., Castelo, A., Cuminato, J.A., Mangiavacchi, N. and McKee, S., 2001. "Gensmac3d: a numerical technique for solving three-dimensional free surface flows". *Int. J. Numer. Methods Fluids*, Vol. 37, pp. 747–796.

Tomé, M.F., Castelo, A., Cuminato, J.A. and McKee, S., 1996a. "Gensmac3d: implementation of the navier-stokes equations and boundary conditions for 3d free surface flows". Notas do ICMC no. 29, Departamento de Ciência de Computação e Estatística, Universidade de São Paulo.

Tomé, M.F., Duffy, B. and McKee, S., 1996b. "A numerical technique for solving unsteady non-newtonian free surface flows". *J. Non-Newtonian Fluid Mech*, Vol. 62, No. 1, pp. 9–34.

Tomé, M.F. and McKee, S., 1994. "Gensmac: A computatinal marker-and-cell method for free surface flows in general domains". *J. Comp. Phys.*, Vol. 110, No. 1, pp. 171–186.

Wang, X., Dong, H., Zhang, X., Yu, L., Zhang, S. and Xu, Y., 2010. "Numerical simulation of single bubble motion in ionic liquids". *Chemical Engineering Science*, Vol. 65, pp. 6036–6047.

Wua, M. and Gharib, M., 2002. "Experimental studies on the shape and path of small air bubbles rising in clean water". *Physics of Fluids*, Vol. 14, pp. 49–52.

Xu, H. and Guetari, C., 2004. "Numerical simulations of a train of air bubbles rising through stagnant water". 13 Jan. 2011 <http://www.ansys.com/events/proceedings/2004.asp>.

Zhang, L., Yang, C. and Mao, Z.S., 2010. "Numerical simulation of a bubble rising in shear-thinning fluids". *J. Non-Newtonian Fluid Mech*, Vol. 165, pp. 555–567.